Electrochemical and Thermal Property Enhancement of Natural Graphite Electrodes via a Phosphorus and Nitrogen Incorporating Surface Treatment

Kyungbae Kim, Han-Seul Kim, Hyungeun Seo, and Jae-Hun Kim[†]

School of Materials Science and Engineering, Kookmin University, Seoul 02707, Republic of Korea

An efficient wet process approach to modifying natural graphite (NG) electrodes for Li-ion batteries is introduced in this paper. With homogeneous mixing and thermal decomposition of NG with diammonium phosphate ($(NH_4)_2HPO_4$), phosphorus and nitrogen were successfully incorporated into the surface layer of NG particles. Electron microscopy and X-ray photoelectron spectroscopy analyses demonstrated that the surface was well modified by this process. As a result, the treated NG electrodes exhibited much improved electrochemical performance over pristine NG at two different temperatures: 25 °C and 50 °C. Excellent capacity retention of 95.6% was obtained after 100 cycles at 50 °C. These enhanced properties were confirmed in a morphology analysis on the cross-sections of the NG electrodes after galvanostatic cycling. The improved cycle and thermal stabilities can be attributed to the surface treatment with phosphorus and nitrogen; the treatment formed a stable solid electrolyte interphase layer that performed well when undergoing Li insertion and extraction cycling.

Keywords: Natural graphite, Surface treatment, Phosphorus and nitrogen incorporation, Solid electrolyte interphase, Lithium battery

1. Introduction

With ever-increasing energy demands, electrochemical energy storage devices have attracted great attention. Among them, Li-ion batteries (LIBs) are considered to be key energy storage media because of their high energy density, good cycle life, and reasonable cost [1]. Research to enhance the properties of LIBs is increasing as LIB applications progress from portable electronics to electric vehicles and energy storage systems. The most important issues facing commercialized LIBs are their cycling and thermal stabilities. Battery performance depends highly on its electrode materials, so the development of superior electrode material is essential.

In currently available commercial LIBs, carbonaceous materials have been widely used as negative electrodes (anodes). Among several carbon-based materials, natural graphite (NG) is one of the most attractive anode materials for LIBs because of its low and flat reaction potential near 0 V (*vs.* Li^+/Li), its relatively high specific capacity

of 372 mA h g^{-1}, and its low cost [2]. However, the use of pure NG in practical Li-ion cell systems is limited due to its poor cycle stability and rate capability resulting from repeated surface exfoliation and decomposition of solid electrolyte interphase (SEI) films during cycling [3-6]. Moreover, the thermal stability of NG is one of the critical issues for commercial applications, because thermal runaway in anodes is a big problem that directly affects the safety of cells [7-9]. The electrochemical and thermal properties of NG depend primarily on its surface SEI layer characteristics [10-12] and therefore effective surface treatments are required.

In this study, we propose an effective method for more stable SEI formation that incorporates phosphorus and nitrogen in the graphite through treatment with diammonium phosphate. The incorporated phosphorus and nitrogen form highly durable SEI layers on the graphite's surface, resulting in enhanced thermal resistivity and electrochemical performance. To examine the performance changes induced by this surface treatment, we carried out electrochemical and structural characterizations at room temperature (25 °C) and high temperature (50 °C). The analysis results demonstrated that the proposed surface treatment can play an important role in enhancing NG

[†]Corresponding author: jaehunkim@kookmin.ac.kr
Kyungbae Kim: 연구교수, Han-Seul Kim: 석사과정,
Hyungeun Seo: 박사과정, Jae-Hun Kim: 교수

anode performance.

2. Experimental Methods

2.1 Materials synthesis

Natural graphite (NG, Alfa Aesar) with a particle size of 2-15 μm was used as the starting material. Diammonium phosphate ($(NH_4)_2HPO_4$, Sigma-Aldrich) solution was used for thermal decomposition in a wet process. For the NG surface treatment, 0.2 g of $(NH_4)_2HPO_4$ and 6 g of NG were dissolved into a 20 mL solution consisting of 15 mL of de-ionized water and 5 mL of ethanol (EtOH). The solution was well mixed for 8 h and then vacuum dried at 110 °C for 4 h. The dried powder was heat-treated at 400 °C for 5 h in an N_2 atmosphere in a typical horizontal furnace.

2.2 Materials characterization

X-ray diffraction (XRD, Rigaku D/MAX-2500V with Cu Kα radiation) patterns of the NG samples were obtained to characterize the crystal structure. The material's molecular bonding structure was analyzed with Raman spectroscopy (Renishaw containing an Nd:YAG laser working at a wavelength of 532 nm). The morphology and microstructure of the materials and electrodes were observed by means of field-emission scanning electron microscopy (FE-SEM, JEOL JSM-7610F) and high-resolution transmission electron microscopy (HR-TEM, JEOL ARM200F) with an energy dispersive spectroscopy (EDS) detector. The chemical state of the surface-treated NG was examined with X-ray photoelectron spectroscopy (XPS, Thermo Scientific Sigma Probe containing Al Kα radiation). To examine the thermal properties of the NG electrodes, differential scanning calorimetry (DSC, Mettler Toledo STARe system) was applied after the full discharge of the pristine NG and surface-treated NG electrodes to 0.001 V vs. Li^+/Li at a temperature range of 25-450 °C and a heating rate of 5 °C min^{-1}.

2.3 Electrochemical measurements

Electrodes were prepared using a slurry-casting method. The coating slurry containing the active material (96 wt%) and binder (CMC/SBR 4 wt%) was dissolved in de-ionized water. The slurry was coated onto copper foils. The coated electrodes were roll-pressed and dried in a vacuum at 80 °C for 12 h. The well-dried electrodes were cut into disks with a diameter of 12 mm. CR2032 coin-type half-cells were assembled using a working electrode, a Li-metal foil as the counter/reference electrode, and a porous polyethylene (PE, SETELA™, Toray Battery Separator Film Inc.) separator; the electrolyte consisted of 1.0 M $LiPF_6$ in ethyl carbonate/diethyl carbonate/ethyl methyl carbonate (EC/DEC/EMC; volume ratio: 3:3:4; Panax Etec) containing 1 wt% vinylene carbonate (VC) and 1 wt% lithium bis(oxalate)borate (LiBOB). Galvanostatic discharge (Li^+ intercalation) and charge (Li^+ de-intercalation) tests were performed using a battery cycler (Maccor Series 4000) at a constant current of 0.1 C (1 C = 370 mA g^{-1}) within the potential windows of 0.001–2.0 V (vs. Li^+/Li) at 25 °C and at 50 °C. The rate performance testing was carried out at constant rates of 0.1, 0.2, 0.5, 1.0, 2.0, and 5.0 C.

3. Results and Discussion

Fig. 1a illustrates the entire surface treatment process. A simple wet immersion process to modify the surface was first applied and then phosphorous and nitrogen incorporation occurred during the thermal decomposition of
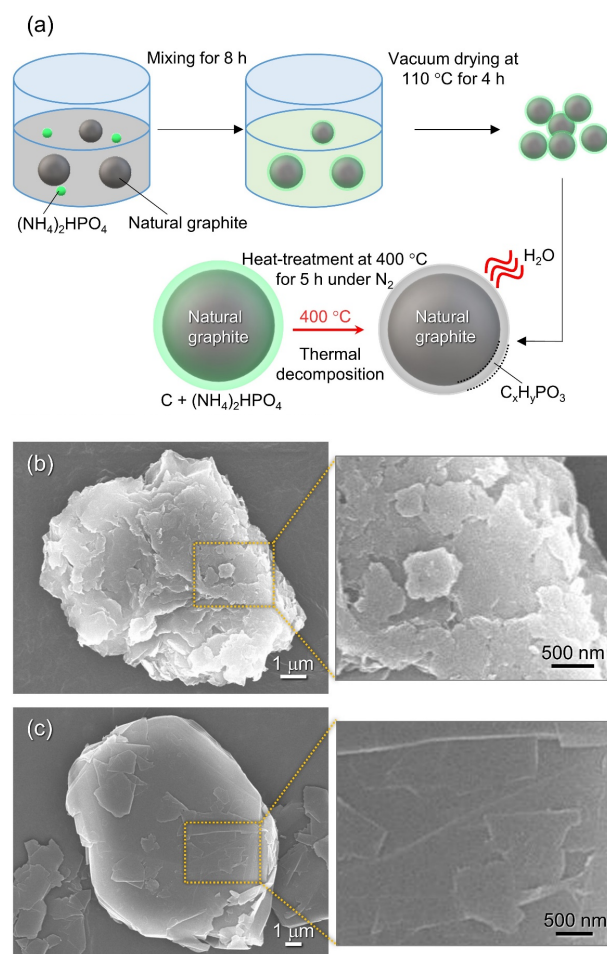

Fig. 1 (a) Schematic illustration of the NG surface treatment process, and FE-SEM images of (b) pristine NG and (c) surface-treated NG particles.

$(NH_4)_2HPO_4$. FE-SEM images of both pristine and surface-treated NG are presented in Fig. 1b and c. A morphology change was clearly observable after surface treatment. The surface of pristine NG appeared as a rough graphite sheet with a particle size of approximately 15 μm (Fig. 1b). After the treatment, the surface became smooth and the graphite particles had round shapes (Fig. 1c).

HR-TEM analysis was performed to find more detailed differences between the microstructures of the pristine and treated NG materials. Fig. 2a shows the HR-TEM image of pristine NG where highly ordered graphene layers are observed in the (002) plane at a d-spacing of 3.388 Å, a typical feature of graphite. In the HR-TEM image of the surface-treated NG (Fig. 2b), an amorphous layer is clearly seen, indicating that the surface changed during the thermal decomposition process. The bulk structure remained unaffected with a d-spacing of 3.391 Å corresponding to the (002) reflection. This indicates that the wet immersion and thermal decomposition treatment achieved modification of only the surfaces of the NG particles.

Crystal and molecular bonding structures of pristine and surface-treated NG were also characterized to examine their differences. Fig. 2c shows the XRD patterns of both materials. All diffraction peaks matched well with the hexagonal structure of NG (JCPDS, No. 41-1487). After surface treatment, no crystal structure change was detected, which means that the surface treatment did not affect the

bulk crystal structure. On the other hand, Raman analysis results exhibited some differences between the pristine and surface-treated NG (Fig. 2d). Both Raman spectra show a typical NG bonding structure with clear D, G, D′, and 2D bands at 1350, 1580, 1620, and 2700 cm^{-1}, respectively [13]. However, their shapes were different. The profile of the surface-treated NG exhibited more broadened G and 2D bands, and stronger D and D′ bands than that of the pristine NG. In particular, D and D′ bands are attributed to a disorder-induced band. Therefore, these changes in bands could have resulted from the amorphous nature of the outermost parts of the surface-treated NG particles. The degree of disorder can be defined as an R-value, which can be written as the ratio of D to G band intensity ($R = I_D/I_G$). The R-values of the pristine NG and surface-treated NG were 0.036 and 0.852. The much greater R-value for the surface-treated NG indicates that the bonding states were greatly changed after the treatment. These Raman results agree well with the HR-TEM analysis.

To investigate the surface chemistry, EDS and XPS analyses were performed on the surface-treated NG; the results are presented in Fig. 3. The layered, C, P, and N EDS elemental mapping images are provided as insets. Fig. 3a shows the XPS survey spectra of the pristine and surface-treated NG. After treatment, signals for P, N, and O elements newly appeared, which indicates that these components were incorporated into the graphite surface during the wet immersion and thermal decomposition
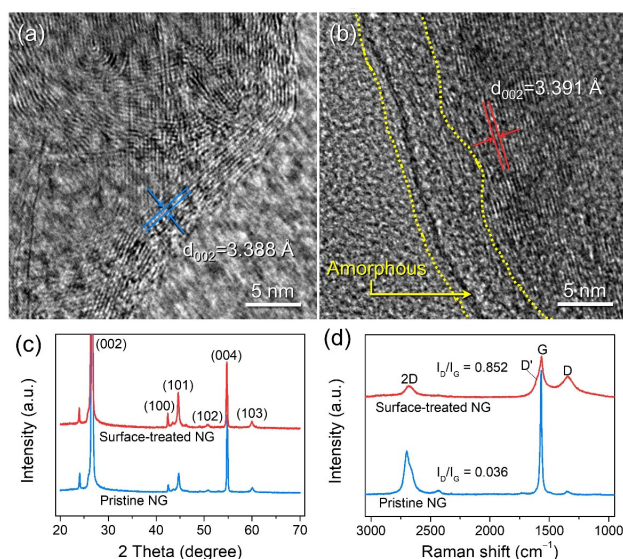

Fig. 2 HR-TEM images of (a) pristine NG and (b) surface-treated NG. (c) XRD patterns and (d) Raman spectra of pristine and surface-treated NG.
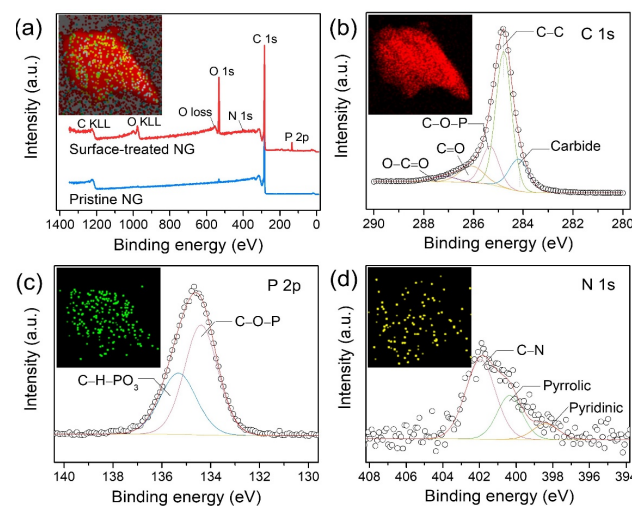

Fig. 3 (a) XPS survey spectra of pristine and surface-treated NG (inset: EDS elemental mapping image of surface-treated NG) and high-resolution core-level photoelectron spectra of surface-treated NG: (b) C 1s, (c) P 2p, and (d) N 1s (inset: EDS mapping images for each component).

processes. Fig. 3b–d display the core-level XPS spectra for C 1s, P 2p, and N 1s. The C 1s spectrum was deconvoluted into five sub-profiles centered at 284.1, 284.6, 285.4, 286.1, and 287.6 eV, which could be attributed to carbide, C–C, C–O–P, C=O, and O–C=O, respectively (Fig. 3b) [14]. Interestingly, the sub-profile of the C–O–P bond is very strong, which could be indicative of phosphorus incorporation from the $(NH_4)_2HPO_4$ treatment. The presence of phosphorus in the surface can be clarified from the P 2p spectrum in Fig. 3c. Two sub-profiles were centered at 134.5 and 135.4 eV, which are generally assigned to phosphate P^{3+} in C–O–P and P^{5+} in pentavalent phosphorus, respectively [15]. The N 1s spectrum was deconvoluted into 3 sub-profiles at 398.2, 400.1, and 401.7 eV, which correspond to pyridinic, pyrrolic, and C–N bonds, respectively. The existence of phosphorus and nitrogen in the surface of NG can stabilize SEI formation as previously indicated in the literature [16-21].

The galvanostatic discharge-charge tests were performed for the pristine and surface-treated NG electrodes at 25 and 50 °C to compare their electrochemical performance and thermal stability. The voltage profiles of the electrodes obtained at 25 °C are shown in Fig. 4a. The first discharge and charge capacities were 412 and 368 mA h g^{-1}, respectively with an initial coulombic efficiency of 89.3% for the pristine electrode. After the treatment, the discharge and charge capacities were 366 and 345 mA h g^{-1}, respectively, with a coulombic efficiency of 94.3%.

The reversible capacity was decreased because some active sites for Li storage were removed by the surface treatment. However, the initial coulombic efficiency was greatly improved because irreversible surface reactions during the first cycle were prevented by the surface modifications. Fig. 4b shows the cycle performance of both electrodes measured at a rate of 0.1 C. The capacity retentions up to 100 cycles were measured to be 68.7 and 83.8% for pristine and surface-treated NG electrodes, respectively. The enhanced cycling stability of the surface-treated electrode can be attributed to its stable SEI layer formation induced by its surface modification.

Fig. 5 shows the electrochemical properties of both the pristine and treated electrodes measured at 50 °C. The cycle performance of both electrodes is given in Fig. 5a. The capacity retention ratios after 100 cycles were 63.9 and 95.6% for pristine and surface-treated NG electrodes. After surface modification, a noticeable enhancement of cycling stability at the high temperature can be seen; this could be attributed to the incorporation of phosphorus and nitrogen. Fig. 5b exhibits the rate capability results of both electrodes at 50 °C. The rate performance at the high temperature was also greatly improved after the treatment. This enhanced electrochemical performance can be attributed to the formation of stable SEI films assisted by phosphorus and nitrogen incorporation. The smooth microstructure of surface-treated NG supports the formation of these films; it is found to be more suitable for fast sol-
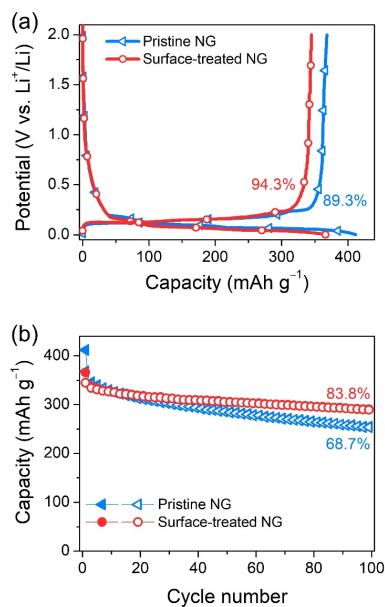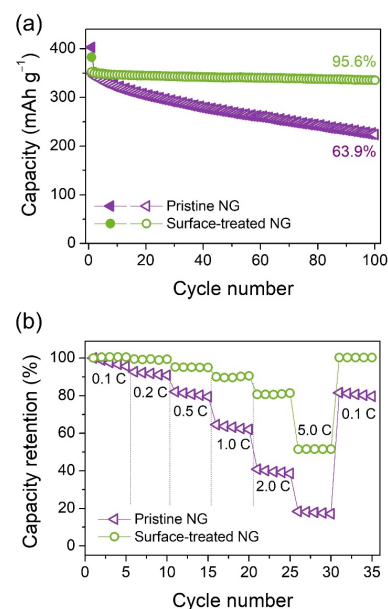

Fig. 4 Electrochemical properties at room temperature (25 °C): (a) voltage profiles and (b) cycle performance of pristine NG and surface-treated NG electrodes at a 0.1 C rate.

Fig. 5 Electrochemical properties at high temperature (50 °C): (a) cycle performance at a 0.1 C and (b) rate performance at various rates for pristine NG and surface-treated NG electrodes.
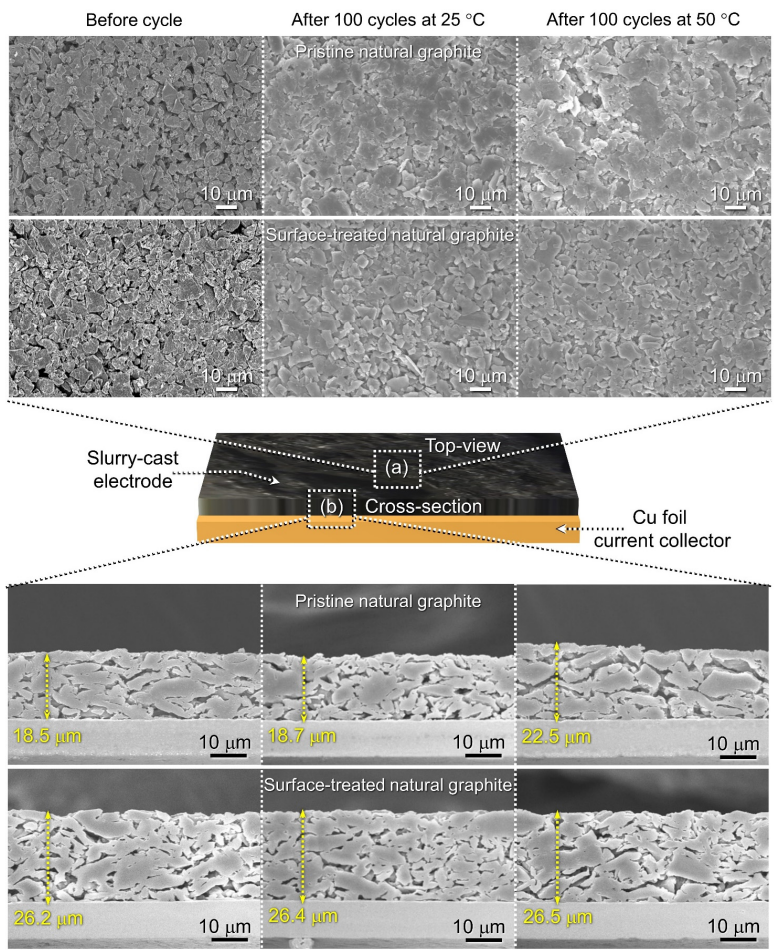
Fig. 6 FE-SEM images of pristine and surface-treated NG electrodes before and after 100 cycles at 25 °C and 50 °C: (a) top view and (b) cross-sectional view.
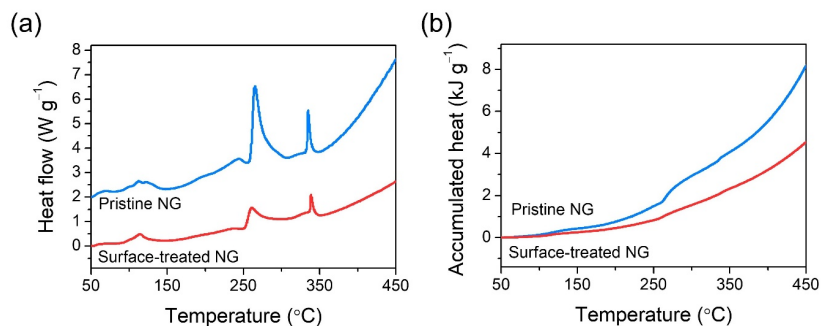

Fig. 7 (a) DSC curves and (b) corresponding accumulated heat flow curves of pristine and surface-treated NG electrode materials.

id-state diffusion and charge transfer at the interface of NG and electrolyte.

The dimensional stability of the electrodes was investigated using FE-SEM analysis after 100 cycles at 25 °C and 50 °C. The surface and cross-sectional FE-SEM images are compared before and after cycling at a rate of

0.2 C in Fig. 6. Before cycling, the top-view and cross-section images of both electrodes exhibited uniform and clear graphite particles, as observed in Fig. 1. After 100 cycles at 25 °C, the particle shape and pores of the surface-treated NG electrode were well maintained, while the pristine NG showed agglomeration on its surfaces.

Similar morphologies were observed even after 100 cycles at 50 °C. In terms of electrode thickness, the pristine NG electrode presented a considerable increase from 18.5 to 22.5 μm, but the surface-treated NG exhibited no noticeable thickness changes. From these results, it can be inferred that the treated surface of NG is resistant to irreversible reactions that consume Li during repeated Li insertion and extraction cycling.

To investigate thermal stability, DSC analysis was performed on both electrode materials and the results are presented in Fig. 7. Both heat flow curves exhibited the general heat flow tendency of graphite materials with two main exothermic peaks at 275 and 348 °C [22]. The surface-treated NG electrode showed smaller heat flow and accumulated heat values than the pristine NG electrode. This reveals that the phosphorus and nitrogen incorporation on the surface of NG is effective in protecting the graphite material from heat. The results correspond well with the cycle performance results at a high temperature.

4. Conclusions

We demonstrated the surface modification of NG material by incorporating phosphorus and nitrogen using simple wet immersion and $(NH_4)_2HPO_4$ thermal decomposition processes. Comprehensive analysis results revealed that the NG surface treatment was successful. The modification led to the formation of stable SEI layers; these layers are essential for the enhancement of NG electrochemical properties. After the treatment, the initial coulombic efficiency of the NG electrode was greatly improved. Moreover, surface-treated NG exhibited much-improved cycle performance and rate capability at a high temperature of 50 °C. It was confirmed by FE-SEM analysis after 100 cycles that the electrode morphology of the surface-treated NG electrode was better than that of the pristine NG electrode. Our simple surface modification treatment can be applied to the development of other functional materials for diverse applications.

Acknowledgments

References

1. N. Nitta, F. Wu, J. T. Lee, and G. Yushin, *Mater. Today*, **18**, 252 (2015).
2. M. Endo, C. Kim, K. Nishimura, T. Fujino, and K. Miyashita, *Carbon,* **38**, 183 (2000).
3. J. M. Tarascon and M. Armand, *Nature*, **414**, 359 (2001).
4. P. Verma, P. Maire, and P. Novak, *Electrochim. Acta*, **55**, 6332 (2010).
5. N. A. Kaskhedikar and J. Maier, *Adv. Mater.* **21**, 2664 (2009).
6. S. Flandrois and B. Simon, *Carbon*, **37**, 165 (1999).
7. Y. P. Wu, E. Rahm, and R. Holze, *J. Power Sources*, **114**, 228 (2003).
8. C. Wang, A. J. Appleby, and F. E. Little, *J. Electroanal. Chem.*, **497**, 33 (2001).
9. T. Waldmann, M. Wilka, M. Kaper, M. Fleischhammer, and M. Wohlfahrt-Mehrens, *J. Power Sources*, **262**, 129 (2014).
10. J.-I. Yamaki, H. Takatsuji, T. Kawamura, and M. Egashira, *Solid State Ionics*, **148**, 241 (2002).
11. A. M. Andersson, D. P. Abraham, R. Haasch, S. MacLaren, J. Liu, and K. Amine, *J. Electrochem. Soc.*, **149**, A1358 (2002).
12. H. Park, T. Yoon, J. Mun, J. H. Ryu, J. J. Kim, and S. M. Oh, *J. Electrochem. Soc.*, **160**, A1539 (2013).
13. J. Xu, I. -Y. Jeon, J. Ma, Y. Dou, S. -J. Kim, J. -M. Seo, H. Liu, S. Dou, J. -B. Baek, and L. Dai, *Nano Res.*, **10**, 1268 (2016).
14. J.-H. Zhou, Z.-J. Sui, J. Zhu, P. Li, D. Chen, Y.-C. Dai, and W.-K. Yuan, *Carbon*, **45**, 785 (2007),
15. A. M. Puziy, O. I. Poddubnaya, R. P. Socha, J. Gurgul, and M. Wisniewski, *Carbon*, **46**, 2113 (2008).
16. C.-M. Park and H.-J. Sohn, *Adv. Mater.* **19**, 2465 (2007).
17. A. Pimenta, G. Dresselhaus, M. S. Dresselhaus, L. G. Cancado, A. Jorio, and R. Saito, *Phys. Chem. Chem. Phys.*, **9**, 1276 (2007).
18. Z. Yu, J. Song, M. L. Gordin, R. Yi, D. Tang, and D. Wang, *Adv. Sci.*, **2**, 1400020 (2015).
19. M.-S. Park, J.-H. Kim, Y.-N. Jo, S.-H. Oh, H. Kim, and Y.-J. Kim, *J. Mater. Chem.*, **21**, 17960 (2011).
20. D. Wei, Y. Liu, Y. Wang, H. Zhang, L. Huang, and G. Yu, *Nano Lett.*, **9**, 1752–1758 (2009).
21. H. Wang, C. Zhang, Z. Liu, L. Wang, P. Han, H. Xu, K. Zhang, S. Dong, J. Yao, and G. Cui, *J. Mater. Chem.*, **21**, 5430 (2011).
22. H. Yang, H. Bang, K. Amine, and J. Prakash, *J. Electrochem. Soc.*, **152**, A73 (2005).